

Zebrafish models for human ALA-dehydratase-deficient porphyria (ADP) and hereditary coproporphyria (HCP) generated with TALEN and CRISPR-Cas9

Shuqing Zhang^{1,2}, Jiao Meng^{1,2}, Zhijie Niu^{1,2}, Yikai Huang², Jingjing Wang^{1,2}, Xiong Su², Yi Zhou³, Han Wang^{1,2*}

¹Center for Circadian Clocks, Soochow University, Suzhou 215123, Jiangsu, China

²School of Biology & Basic Medical Sciences, Medical College, Soochow University, Suzhou 215123, Jiangsu, China ³Stem Cell Program and Division of Pediatric

Hematology/Oncology, Boston Children's Hospital and Dana Farber Cancer Institute, Harvard Medical School, Boston, MA 02115, USA.

* To whom correspondence should be addressed at: Han Wang, Center for Circadian Clocks, Soochow University, 199 Renai Road, Suzhou, Jiangsu 215123, China. Tel: +86 51265882115; Fax: +86 51265882115; Email: han.wang88@gmail.com or wanghan@suda.edu.cn

Running title: Zebrafish models for human porphyrias ADP and HCP

ABSTRACT: Defects in the enzymes involved in heme biosynthesis result in a group of human metabolic genetic disorders known as porphyrias. Using a zebrafish model for human hepatoerythropoietic porphyria (HEP), caused by defective uroporphyrinogen decarboxylase (Urod), the fifth enzyme in the heme biosynthesis pathway, we recently have found a novel aspect of porphyria pathogenesis. However, no heritable zebrafish models with genetic mutations of *alad* and *cpox*, encoding the second enzyme delta-aminolevulinate dehydratase (Alad) and the sixth enzyme coproporphyrinogen oxidase (Cpox), have been established to date. Here we employed site-specific genome-editing tools transcription activator-like effector nuclease (TALEN) and clustered regularly interspaced short palindromic repeats (CRISPR)/CRISPR-associated protein 9 (Cas9) to generate zebrafish mutants for *alad* and *cpox*. These zebrafish mutants display phenotypes of heme deficiency, hypochromia, abnormal erythrocytic maturation and accumulation of heme precursor intermediates, reminiscent of human ALA-dehydratase-deficient porphyria (ADP) and hereditary coproporphyrin (HCP), respectively. Further, we observed altered expression of genes involved in heme biosynthesis and degradation and particularly down-regulation of exocrine pancreatic zymogens in ADP (*alad*^{-/-}) and HCP (*cpox*^{-/-}) fishes. These two zebrafish porphyria models can survive at least 7 days and thus provide invaluable resources for elucidating novel pathological aspects of porphyrias, evaluating mutated forms of human *ALAD* and *CPOX*, discovering new therapeutic targets and developing effective drugs for these complex genetic diseases. Our studies

46 also highlight generation of zebrafish models for human diseases with two versatile

47 genome-editing tools.

48

49 **Keywords:** Zebrafish, heme, porphyria, *alad*, *cpox*, TALEN, CRISPR-Cas9

50

51

52 **Introduction**

53 The porphyrias are a group of rare and clinically complex metabolic disorders, each
 54 caused by genetic mutations that result in defective enzymes involved in eight highly
 55 conserved reactions of heme biosynthesis (Balwani and Desnick, 2012; Puy et al.,
 56 2010). Deficiencies of the second enzyme delta-aminolevulinate dehydratase (ALAD;
 57 EC 4.2.1.24) in the heme biosynthesis pathway cause autosomal recessive
 58 ALA-dehydratase-deficient porphyria (ADP; Online Mendelian Inheritance in Man,
 59 OMIM 125270, John Hopkins University, Baltimore, MD) (Jaffe and Stith, 2007; Yano
 60 and Kondo, 1998); whereas deficiencies of the sixth enzyme coproporphyrinogen
 61 oxidase (CPOX, EC 1.3.3.3) lead to autosomal dominant hereditary coproporphyria
 62 (HCP; OMIM 121300) (Whatley et al., 2009). Both porphyrias are acute hepatic and
 63 clinically manifest neurologic attacks, abdominal pain, nausea, vomiting, tachycardia,
 64 and hypertension (Siegesmund et al., 2010). The diagnosis of the two porphyrias is
 65 primarily through detection of elevated levels of delta-aminolevulinic acid (ALA),
 66 coproporphyrin III and porphobilinogen (PBG) in urine, feces and blood, combined
 67 with enzymatic assays and mutation analysis (Balwani and Desnick, 2012; Cappellini
 68 et al., 2010; Maruno et al., 2001; Puy et al., 2010).

69 The zebrafish (*Danio rerio*) has been a model for investigating molecular genetic
 70 mechanisms underlying numerous human disorders including hematopoietic diseases
 71 (Dooley and Zon, 2000; Lieschke and Currie, 2007), and also has been particularly
 72 effective for high-throughput drug screens in whole organism (MacRae and Peterson,
 73 2015; North et al., 2007; Pouretezadi et al., 2014; Rennekamp and Peterson, 2015;

74 Zon and Peterson, 2005). Using a zebrafish model for human hepatoerythropoietic
 75 porphyria (HEP; OMIM 176100) (Wang et al., 1998), we recently have uncovered a
 76 novel aspect of porphyric pathogenesis, i.e., heme regulates exocrine pancreatic
 77 zymogens through the Bach1b/Nrf2a-MafK pathway (Wang et al., 2007; Zhang et al.,
 78 2014), demonstrating that the utilities and power of zebrafish disease models for
 79 delineating novel pathogenesis mechanisms (Santoriello and Zon, 2012). However, no
 80 heritable zebrafish *alad* and *cpox* models with genetic mutations have been generated
 81 to date. A medaka (*Oryzias latipes*) *whiteout* (*who*) mutant was previously
 82 characterized as a model for human ADP based upon its phenotype of hypochromic
 83 anemia (Sakamoto et al., 2004), but medaka spawns relative fewer eggs (20~40) each
 84 time (Furutani-Seiki and Wittbrodt, 2004) and has not yet been developed for
 85 large-scale drug screens. Even though *cpox*-Morpholino-injected zebrafish embryos
 86 were reported as an *in vivo* assay system for assessing biological activities of human
 87 *CPOX* mutations (Hanaoka et al., 2006), these *cpox* morphants are not genetically
 88 stable and particularly difficult to scale up for drug discoveries. A Nakano mouse
 89 displays reduced CPOX enzymatic activities resulted from a *Cpox* mutation (Mori et
 90 al., 2013), however, the Nakano mouse also harbors another mutation in the *Crybg3*
 91 gene tightly linked with *Cpox* on mouse chromosome 16. Thus the Nakano mouse also
 92 manifests cataracts that human HCP patients do not develop, whereby compounding its
 93 phenotype and limiting its use in investigating novel aspects of porphyria pathogenesis.
 94 Hence, zebrafish *alad* and *cpox* genetic models are needed.

95 Transcription activator-like effector nuclease (TALEN) and clustered regularly
 96 interspaced short palindromic repeats (CRISPR)/CRISPR-associated protein 9 (Cas9)
 97 are two site-specific genome-editing systems, each composed of a DNA-recognizing
 98 component and a DNA-cleavage component (Hwang et al., 2013; Irion et al., 2014;
 99 Wei et al., 2013). In the TALEN system, the two TALE domains are the
 100 DNA-recognizing component and the two FokI domains are the DNA-cleavage
 101 component (Huang et al., 2014), while in the CRISPR-Cas9 system, the single
 102 guide-RNA (gRNA) is in charge of DNA-recognizing and the Cas9 endonuclease in
 103 charge of DNA-cleavage (Hsu et al., 2014). A pair of TALENs or one gRNA along
 104 with the Cas9 protein suffice to generate site-specific DNA double-strand breaks
 105 (DSBs) that trigger the endogenous nonhomologous end joining (NHEJ) DNA repair
 106 pathway to induce indel mutations in targeted genes in numerous species including
 107 zebrafish (Cong and Zhang, 2015; Wei et al., 2013).

108 Here we used TALEN and CRISPR-Cas9 to generate zebrafish mutants for *alad* and
 109 *cpox*. Characterization of these two zebrafish mutants found that they both manifest
 110 phenotypes of heme deficiency, hypochromia, abnormal erythrocytic maturation and
 111 accumulation of heme precursor intermediates, and in particular that *cpox* mutants
 112 display reddish autofluorescence, resembling human ALA-dehydratase-deficient
 113 porphyria (ADP) and hereditary coproporphyrin (HCP), respectively. These zebrafish
 114 new models of human porphyrias are invaluable for elucidating novel pathological
 115 aspects of porphyrias, in vivo assessments of mutations of these human disease genes,

116 discovering new therapeutic targets and developing effective drugs for these complex
117 genetic diseases.

118

119 **Results**

120 **Generation of zebrafish *alad* mutants with TALEN**

121 A pair of TALENs was designed to target exon 3 of zebrafish *alad*
122 (ENSDARG00000052815) with a BsmA I restriction endonuclease site in the targeted
123 fragment for subsequent mutant identification (Fig. 1A). Following microinjection of
124 this pair of *alad* TALEN mRNAs into single-cell zebrafish embryos, we extracted
125 DNAs from injected and control embryos. By PCR amplification and restriction
126 endonuclease digestion analysis, we estimated a mutagenesis rate of approximately
127 44% in F₀ embryos (Fig. S1A). To identify the induced mutation types, the uncleaved
128 DNA fragments were then cloned and sequenced. Sequencing results showed that there
129 are several types of deletions in the targeted fragment (Fig. 1B) (Xiao et al., 2013). The
130 remaining F₀ fish were raised to adulthood and then crossed with wild-type fish to
131 produce F₁. To screen for inheritable mutations, DNAs extracted from approximately
132 10 F₁ embryos of each cross were used for PCR amplification and enzymatic digestion
133 analysis. The germline transmission efficiency of *alad* TALEN-induced mutations was
134 estimated to be approximately 20% (Supplementary Table S1). Siblings of the F₁ fish
135 carrying inheritable mutations were raised to adulthood and re-identified by PCR,
136 restriction endonuclease digestion and sequencing of fin-clipped DNAs. An *alad*
137 mutant line carrying a 14-bp deletion resulting in a frame shift starting the 51th amino

138 acid (ZFIN allele nomenclature designation, *alad*^{*sus003*}) (Fig. 1C) was used for the
 139 further experiments.

140 **Generation of zebrafish *cpx* mutants with CRISPR-Cas9**

141 To generate zebrafish mutants for *cpx* (ENSDARG00000062025), we selected a 20-nt
 142 gRNA immediate to a PAM (protospacer adjacent motif) sequence (NGG) located at
 143 exon 2 of *cpx*, and the targeted fragment also contains a Hinf I restriction
 144 endonuclease site for subsequent genotyping (Fig. 1D). Single-cell zebrafish embryos
 145 were microinjected with the synthetic Cas9 mRNA and *cpx* gRNA. DNAs extracted
 146 from injected and control embryos were PCR amplified. Restriction endonuclease
 147 digestion of the PCR products detected approximately 44% to 49% of mutagenesis
 148 frequency induced by gRNA-Cas9 (Fig. S1B). Cloning and sequencing of the
 149 uncleaved DNA fragments showed several types of small deletions adjacent to PAM in
 150 F₀ embryos (Fig. 1E). The remaining F₀ embryos were raised to adulthood. DNAs
 151 extracted from the F₁ embryos produced by crossing F₀ fish with wild-type fish were
 152 PCR amplified. Restriction endonuclease digestion of the PCR products identified the
 153 corresponding F₀ fish carrying inheritable mutations. The germline transmission
 154 efficiency of the *cpx* CRISPR/Cas9-induced mutations was approximately 17%
 155 (Supplementary Table S1). Siblings of the F₁ fish identified as carrying inheritable
 156 mutations were raised to adulthood and re-identified by PCR, restriction endonuclease
 157 digestion and sequencing of fin-clipped DNAs. Two *cpx* mutant lines, one harboring a
 158 6-bp deletion resulting in deletion of 2 amino acids (ZFIN allele nomenclature
 159 designation, *cpx*^{*sus004*}) in a highly conserved region (Hanaoka et al., 2006) and the

160 other possessing a 11-bp deletion resulting in a truncated peptide with only 208 amino
161 acids (ZFIN allele nomenclature designation, *cpox*^{sus005}), were identified (Fig. 1F).
162 These two *cpox* mutant fishes display similar phenotypes and were used in the
163 following experiments.

164 **Zebrafish *alad*^{-/-} and *cpox*^{-/-} mutants display severe hypochromic anemia**

165 The *alad*^{-/-} and *cpox*^{-/-} mutant embryos exhibit hypochromic phenotype as early as 48
166 hours post fertilization (hpf) (Fig. 2A). The circulating blood cells of the wild-type
167 pericardia are reddish, while those of the *alad*^{-/-} and *cpox*^{-/-} mutant pericardia are pale
168 (Fig. 2A). In addition, the *cpox*^{-/-} mutant displays reddish autofluorescence (see the
169 result below), presumably due to the excessive accumulation of photosensitive
170 porphyrin. Although heterozygous *alad*^{+/-} and *cpox*^{+/-} fish appear unaffected
171 outwardly and can grow to adulthood, homozygous embryos die due to severe
172 embryonic anemia. The mass death of *alad*^{-/-} homozygotes starts at 7 dpf, and their
173 survival rate drops to 0% at 14 dpf (Fig. 2D), suggesting that *alad*^{-/-} homozygous
174 larvae cannot survive longer than 13 days. The mass death of *cpox*^{-/-} starts at 6 dpf, and
175 *cpox*^{-/-} homozygous larvae cannot survive longer than 11 days (Fig. 2D). Homozygous
176 *alad*^{-/-} and *cpox*^{-/-} larvae that survive past day 10 (Fig. 2B) are pale, and have much
177 shorter body length (Fig. 2C) but do not have observable ingested food in the intestine
178 compared to wild-type control larvae (Fig. 2B).

179 **Abnormal erythrocytic maturation in *alad*^{-/-} and *cpox*^{-/-} mutant larvae**

180 Whole-mount *in situ* hybridization and qRT-PCR show the expression of *slc4a1a*, a
181 terminal erythroid marker gene, significantly down regulated in *alad*^{-/-} and *cpox*^{-/-}

182 mutants (Fig. 2E, F and G), suggesting insufficient erythroid cells in these two
 183 porphyric mutant zebrafish. Whole-embryo *o*-dianisidine staining also revealed that the
 184 hemoglobin contents of blood cells are severely reduced in *alad*^{-/-} and *cpox*^{-/-} mutants
 185 compared with wild types. Hemoglobin of wild-type embryos is distributed widely in
 186 the ventral part of the yolk from 32hpf to 72hpf (Fig. 3A, D and G), while that of *alad*^{-/-}
 187 (Fig. 3B, E and H) and *cpox*^{-/-} (Fig. 3C, F and I) mutant embryos can be observed only
 188 in a small and narrow area and is markedly reduced compared with wild types (Fig. 3J).
 189 We also performed the hematoxylin-eosin (HE) staining after *o*-dianisidine staining.
 190 Results show that blood cells in *alad*^{-/-} and *cpox*^{-/-} lack the red color of *o*-dianisidine
 191 staining signal compared with wild-type blood cells, suggesting loss of hemoglobin in
 192 these two porphyric mutant zebrafish (Fig. S2A). The blood cell density in section
 193 slides is also significantly reduced in *alad*^{-/-} and *cpox*^{-/-} (Fig. S2B), suggesting the
 194 number of blood cells is significantly decreased in *alad*^{-/-} and *cpox*^{-/-}.

195 Wright staining of circulating embryonic red blood cells showed absence of
 196 acidophilic materials (Fig. 3L-T), especially the cytoplasm in *alad*^{-/-} does not show any
 197 red color at 108 hpf (Fig. 3S). Blood smears assay showed that blood cells of *alad*^{-/-}
 198 and *cpox*^{-/-} mutants have larger nuclei compared with wild-type cells at 72 hpf and 108
 199 hpf (Fig. 3U), suggesting that the erythrocytes of the two mutants differentiate
 200 abnormally.

201 Furthermore, heme contents of the circulating embryonic red blood cells are
 202 significantly reduced in *alad*^{-/-} and *cpox*^{-/-} mutants than wild types (Fig. 3V), and the
 203 mRNA levels of *hbae1* and *hbbe2*, encoding α_{e1} -globin and β_{e2} -globin, are significantly

204 down-regulated in *alad*^{-/-} and *cpox*^{-/-} mutant fishes (Fig. 3K), indicating that heme
205 biosynthesis is disrupted in *alad*^{-/-} and *cpox*^{-/-} mutants, and subsequently leading to the
206 reduced hemoglobin (Tahara et al., 2004a; Tahara et al., 2004b) and abnormal
207 erythrocyte differentiation.

208 **Homozygous *alad*^{-/-} and *cpox*^{-/-} fishes resemble ADP and HCP**

209 The substrate of aminolevulinic acid dehydrase (Alad) is porphyrin precursor
210 δ-aminolevulinic acid (ALA), which normally does not accumulate in significant
211 amounts. The hepatic porphyrias are characterized by overproduction and
212 accumulation of ALA (Cappellini et al., 2010; Costa et al., 1997; Puy et al., 2010; Yano
213 and Kondo, 1998). HPLC (high-performance liquid chromatography) assays showed
214 excessive amounts of ALA in *alad*^{-/-} embryos compared with wild-type embryos (Fig.
215 4A), indicative of defective Alad in the *alad*^{-/-} mutant. In *cpox*^{-/-}, the reddish
216 autofluorescence of the blood cells can be observed in the yolk as early as 30hpf (Fig.
217 4C, D), and HPLC assays also showed excessive amounts coproporphyrinogen
218 III (CP), the substrate of coproporphyrinogen oxidase (Cpox), in *cpox*^{-/-} embryos
219 compared with wild types, indicating the excessive accumulation of photosensitive
220 coproporphyrinogen III of the heme biosynthesis pathway.

221 To determine whether *alad* mRNA or *cpox* mRNA can rescue the phenotypes of
222 *alad*^{-/-} or *cpox*^{-/-} mutant fishes, we microinjected these mRNAs into the mutant and
223 wild-type control embryos (Fig. 5). *o*-Dianisidine staining showed that the hemoglobin
224 content was increased to 60% of the normal level in *alad*^{-/-} and 80% in *cpox*^{-/-}
225 following mRNA microinjection, indicating that the hypochromic anemia phenotype of

226 *alad*^{-/-} and *cpox*^{-/-} is resulted from the mutated *alad* or *cpox* genes. . Taken together,
 227 homozygous *alad*^{-/-} and *cpox*^{-/-} fishes display phenotypes of hypochromia, heme
 228 deficiency, abnormal erythrocytic maturation and accumulation of heme precursor
 229 intermediates, mimicking human ALA-dehydratase-deficient porphyria (ADP) and
 230 hereditary coproporphyrin (HCP).

231 **Evaluating the mutated forms of human ALAD and CPOX in homozygous *alad*^{-/-}**
 232 **and *cpox*^{-/-} fishes**

233 The zebrafish Alad and CpoX proteins are highly similar in sequence to human and
 234 mouse counterparts (Fig. S3) (Hanaoka et al., 2006). In order to examine whether the
 235 biological activities of these two enzymes are conserved between zebrafish and human,
 236 *alad*^{-/-} and *cpox*^{-/-} embryos were microinjected with human *ALAD* or *CPOX* mRNAs
 237 at one-cell stage, respectively. *o*-Dianisidine staining showed that hemoglobin was
 238 significantly increased after injection compared with the mutant embryos without
 239 injection at 48hpf (Fig. 5), indicating that the hypochromic anemia phenotype of *alad*^{-/-}
 240 and *cpox*^{-/-} also can be rescued by human *ALAD* and *CPOX*. In contrast, microinjected
 241 with mutated forms of human *ALAD* or *CPOX* mRNAs from the ADP and HCP patients
 242 (Ishida et al., 1992; Rosipal et al., 1999) did not show any rescue effect (Fig. 5). These
 243 results suggest that the functions of these two enzymes are conserved between
 244 zebrafish and human, and we are able to effectively use homozygous *alad*^{-/-} and
 245 *cpox*^{-/-} fishes to evaluate mutations of these two human disease genes.

246

247 **Expression patterns of genes involved in heme biosynthesis and degradation, and**
 248 **exocrine pancreatic zymogens are disrupted in ADP (*alad*^{-/-}) and HCP (*cpox*^{-/-})**
 249 **fishes**

250 The heme biosynthesis pathway is tightly regulated, and in particular heme
 251 negatively regulates the first and rate-limiting enzyme *Alas1* in the pathway in
 252 non-erythroid cells (Furuyama et al., 2007). qRT-PCR analysis showed that *alas1* is
 253 up-regulated in both ADP and HCP fishes (Fig. 6A, B), likely resulted from heme
 254 deficiencies caused by *alad* and *cpox* mutations. In contrast, heme can enhance its own
 255 synthesis in erythroid cells by up-regulating *alas2* (Chiabrando et al., 2014), and we
 256 observed two *hmbs* (encoding the third enzyme Hmbs in the heme biosynthesis
 257 pathway) genes, *hmbsa* and *hmbsb* in zebrafish (data not shown). While *alas2* and
 258 *hmbsa* are up-regulated but *alad* itself and *hmbsb* are down-regulated in ADP larvae
 259 (Fig. 6A), all genes including upstream and downstream of *cpox* except *ppox* are
 260 up-regulated in HCP larvae (Fig. 6B).

261 Heme oxygenase (Hmox) is the rate-limiting enzyme of the heme degradation
 262 pathway, and can be induced by heme and the oxidative stress of organisms (Applegate
 263 et al., 1991; Igarashi and Sun, 2006). Zebrafish contain three *hmox* genes, *hmox1*,
 264 *hmox2a* and *hmox2b*. While *hmox1*, *hmox2a* and *hmox2b* are up-regulated in HCP
 265 larvae, only *hmox2a* is up-regulated in ADP larvae (Fig. 6C), indicating high levels of
 266 the oxidative stress in these two mutants especially in HCP larvae, likely due to
 267 accumulation of intermediate products of the heme biosynthesis pathway.

Our previous studies found that heme deficiencies result in down-regulation of six peptidase precursor genes in the zebrafish exocrine pancreas (Wang et al., 2007; Zhang et al., 2014). Here qRT-PCR analysis showed that all the six zymogens are also down-regulated in both ADP and HCP larvae (Fig. 6D), providing strong support for our previous finding (Wang et al., 2007; Zhang et al., 2014).

Complex syndromes in different zebrafish porphyria models

Porphyrias show a group of complex syndromes, characteristic of diverse clinical manifestations (Balwani and Desnick, 2012; Cappellini et al., 2010; Puy et al., 2010). We also observed diverse phenotypes in the four zebrafish porphyria models with defective Urod (Wang et al., 1998), CpoX (this study), PpoX (Dooley et al., 2008) and Fech (Childs et al., 2000). First, different autofluorescence patterns can be observed in these four zebrafish heme-deficient models (Fig. 4E-4N). Reddish fluorescence displays primarily in blood cells and internal organs of HEP (*urod*^{-/-}) larvae (Fig. 4H), primarily in the internal organs and yolk of HCP (*cpoX*^{-/-}) (Fig. 4J) and VP (*ppoX*^{-/-}) larvae (Fig. 4L), and in the whole body, especially in the lens, brain and liver of EPP (*feh*^{-/-}) larvae (Fig. 4N). Second, light-induced pericardial edemata have been observed in HEP (*urod*^{-/-}) larvae but not other heme-deficient zebrafish models. As shown in Fig. S4, the appearance of HEP (*urod*^{-/-}) larvae protected under dark condition are normal, while HEP (*urod*^{-/-}) larvae under light exposure display an exacerbating pericardial edema phenotype from 72 hpf to 144 hpf, which cannot be observed in HCP (*cpoX*^{-/-}) larvae. The distinct patterns of reddish fluorescence and light-induced pericardial edemata may be resulted from accumulation of different

290 porphyrins or porphyrin precursors, and these mutants provide tools for reveal the
291 complex pathological mechanisms of human porphyrias.

292

293 **Discussion**

294 Zebrafish have become a bona fide vertebrate model for studying numerous
295 human diseases (Dooley and Zon, 2000; Lieschke and Currie, 2007). Heme
296 biosynthesis is conserved throughout vertebrate evolution (Detrich et al., 1995), all 8 of
297 human genes involved in heme biosynthesis pathway have zebrafish orthologues (Tzou
298 et al., 2014). Four zebrafish mutants *sauternes/alas2* (Brownlie et al., 1998),
299 *yquem/urod* (Wang et al., 1998), *montalcino/ppox* (Dooley et al., 2008) and
300 *dracula/fech* (Childs et al., 2000) were identified in large-scale forward genetic
301 mutagenesis screens (Ransom et al., 1996; Weinstein et al., 1996). A knock-in mouse
302 carrying human *UROS* P248Q missense mutation (*Uros*^{mut248}) represents a model of the
303 congenital erythropoietic porphyria (CEP) (Ged et al., 2006), *Pbgd*-deficient mice
304 generated by gene targeting was reported to exhibit the typical biochemical
305 characteristics of human acute intermittent porphyria (AIP) (Ged et al., 2006; Lindberg
306 et al., 1996), a *URO-D*^{+/-} mouse was generated by homologous recombination as a
307 model of familial porphyria cutanea tarda (PCT) (Phillips et al., 2001), a South African
308 variegate porphyria (VP) mouse model was generated by knocking in the human R57W
309 mutation (Medlock et al., 2002; Meissner et al., 1996), and a BALB/c *Fech*^{m1Pas} mouse
310 was generated by a mutagenesis screen using ethylnitrosourea (ENU) as a model of
311 erythropoietic protoporphyria (EPP) (Tutois et al., 1991)(Table 1). Nevertheless,

312 zebrafish models for ALA-dehydratase deficient porphyria (ADP), acute intermittent
 313 porphyria (AIP), congenital erythropoietic porphyria (CEP) and hereditary
 314 coproporphyria (HCP) have not been reported to date. Here, we generated two
 315 zebrafish models for ADP and HCP with TALEN and CRISPR-Cas9, respectively. Our
 316 work emphasizes that the engineered endonucleases (EENs) TALEN and
 317 CRISPR-Cas9 are efficient tools to generate mutations in zebrafish as models for
 318 heritable human disease.

319 Our studies of *alad*^{-/-} and *cpox*^{-/-} mutants demonstrate that defects in Alad or
 320 Cpx cause hypochromic anemia and abnormal erythrocytic maturation in zebrafish.
 321 The accumulation of ALA and CP, the metabolic intermediates, in the heme synthetic
 322 pathway in *alad*^{-/-} and *cpox*^{-/-} mutants (Fig. 4A, B) indicates that Alad and Cpx
 323 enzymatic activities are impaired by these mutations. Expression of the genes involved
 324 in the heme biosynthetic pathway is altered in *alad*^{-/-} and *cpox*^{-/-}, which may be caused
 325 by the accumulation of metabolic intermediates and/or heme deficiency. The heme
 326 oxygenases participate in the cellular defense from the oxidative damage of reactive
 327 oxygen species (ROS) generated by heme precursors (Ryter and Tyrrell, 2000).
 328 Although heme levels were reduced in *alad*^{-/-} and *cpox*^{-/-}, the heme-induced heme
 329 oxygenase genes were up-regulated likely due to the increased level of oxidative stress.
 330 Interestingly, consistent with our previous finding of heme deficiency-induced
 331 down-regulation of exocrine pancreatic zymogens (Wang et al., 2007; Zhang et al.,
 332 2014), all these six exocrine pancreatic zymogens are significantly down-regulated in
 333 ADP (*alad*^{-/-}) and HCP (*cpox*^{-/-}) fishes (Fig. 6D).

334 Most of the reported human ADP patients are compound heterozygous or
 335 heterozygous, with point mutations of *ALAD* gene resulting in amino acid changes and
 336 reduced enzyme activity (Ishida et al., 1992; Maruno et al., 2001). For the HCP
 337 patients, most are heterozygotes with reduced enzymatic activities and homozygotes
 338 are rare (Kuhnel et al., 2000; Lamoril et al., 1995; Nordmann et al., 1983). The
 339 enzymatic activities of human ALAD or CPOX were investigated through *in vitro*
 340 expression of mutated genes from patients (Martasek et al., 1997; Maruno et al., 2001).
 341 Our rescue experiments showed that the biological activities of these two enzymes are
 342 conserved between zebrafish and human (Fig. 5), these homozygous zebrafish provided
 343 *in vivo* tools for evaluating these human mutated enzymes.

344 Reddish fluorescence was observed in *cpox*^{-/-} embryos under an epifluorescent
 345 stereomicroscope using a rhodamine filter (Fig. 4D). We found that four
 346 heme-deficient zebrafish mutants exhibit distinct patterns of autofluorescence in
 347 different organs (Fig. 4E-N), indicating the complex syndromes and distinct underlying
 348 pathological mechanisms in different types of porphyrias. All eight types of porphyrias
 349 have animal models, providing invaluable resources to study the pathogenesis of
 350 human porphyrias, and six of them are zebrafish models thus far (Table 1). Circulating
 351 blood cells of ADP (*alad*^{-/-}) and HCP (*cpox*^{-/-}) fish lack red color, characteristic of
 352 hypochromic anemia in zebrafish, which can be observed as early as 48 hpf. Moreover,
 353 both of these two homozygous mutants can live at least 7 days, providing a time
 354 window for using these zebrafish models to investigate novel aspects of porphyria
 355 pathogenesis.

356 Zebrafish have been employed as an ideal vertebrate model organism for
 357 high-throughout drug screens and development in whole organism (MacRae and
 358 Peterson, 2015; North et al., 2007; Rennekamp and Peterson, 2015; Zon and Peterson,
 359 2005). The adult heterozygous zebrafish with deficiencies of *alad* or *cpox* can spawn a
 360 large number of embryos each week, homozygous mutant embryos can be easily
 361 identified according to conspicuously pale blood cells (Fig. 2, Fig. S4), and the *cpox*^{-/-}
 362 homozygous embryos even can be identified as early as 32 hpf according to
 363 autofluorescent traits under an epifluorescent stereomicroscope (Fig. 4), which all can
 364 facilitate high-throughput chemical screening for discovering of potential drugs for
 365 preventing or ameliorating the similar symptoms of ADP and HCP in humans. Potential
 366 drugs can be dissolved in the embryo medium and the extent of recovery phenotypes
 367 can be easily detected also through *o*-dianisidine staining (Fig. 5), which provide an
 368 effective assay for drug screening for human porphyrias using these two zebrafish
 369 models.

370 **Materials and Methods**

371 **Fish husbandry and embryo production**

372 The Soochow University Animal Use and Care Committee approved all animal
 373 protocols. Zebrafish wild-type AB strain, and mutant line *alad*^{-/-}, *cpox*^{-/-}, *urod*^{-/-}
 374 (Wang et al., 1998), *ppox*^{-/-} (Dooley et al., 2008) and *fech*^{-/-} (Childs et al., 2000) are
 375 raised at the Soochow University Zebrafish Facility. Wild-type (WT) and mutant
 376 embryos were produced by pair mating, collected for RNA isolation at specified stages.
 377 Homozygous mutants were obtained by mating heterozygous fish and then identified

under an epifluorescent stereomicroscope (Leica M165 FC). The zebrafish mutant lines *alad* and *cpox* generated in this study (See below) have been deposited in both the China Zebrafish Resource Center (CZRC, <http://en.zfish.cn/>) and the Zebrafish International Resource Center (ZIRC, <http://zebrafish.org/home/guide.php>), and the *alad* mutant ZFIN allele nomenclature ID is *alad*^{sus003} (14-bp deletion), and the *cpox* ZFIN allele nomenclature mutant IDs are *cpox*^{sus004} (6-bp deletion) and *cpox*^{sus005} (11-bp deletion), respectively.

***alad*-TALEN construction and microinjection**

The TALEN sites targeting the third exon of zebrafish *alad* were designed using a web-tool TALEN-NT (<https://boglab.plp.iastate.edu/>) (Doyle et al., 2012). TALEN expression vectors were constructed using the ‘Unit Assembly’ method with Sharkey-AS and Sharkey-R forms of FokI cleavage domains as described previously (Huang et al., 2014), were linearized by NotI and used as templates for TALEN mRNA synthesis with SP6 mMESSAGE mMACHINE Kit (Ambion). TALEN mRNAs encoding each monomer were injected in pair into one-cell zebrafish embryos at concentrations of 300 pg. Primers for amplifying the TALEN-targeted fragment are listed in Supplementary Table S2.

***cpox*-gRNA construction and microinjection**

A 20-nt gRNA was selected to target exon 2 of zebrafish *cpox*. The PCR primers for the generation of the DNA template for *cpox*-gRNA were designed, and a T7 promoter sequence was added to 5’upstream of the gRNA sequence. Cas9 mRNA and gRNA were synthesized as described previously (Hwang et al., 2013). Briefly, the Cas9

mRNA was synthesized by *in vitro* transcription using T7 mMESSAGE mMACHINE Kit (Ambion). The gRNA was *in vitro* transcribed and purified using T7 Riboprobe Systems (Promega). Approximately 300 pg of Cas9 mRNA and 75 pg of gRNA were co-injected into one-cell zebrafish embryos. Primers for amplifying the CRISPR-Cas9 targeted fragment are listed in Supplementary Table S2.

RNA isolation and quantitative RT (Real Time)-PCR

Total RNAs were extracted from approximately 20-30 larvae with the TRIzol® Reagent according to the manufacturer's instructions (Invitrogen). The cDNAs synthesized by reverse transcription with the M-MLV reverse transcription kit (Invitrogen) were used as template for quantitative RT-PCR (qRT-PCR) analysis. qRT-PCRs were carried out with the ABI StepOnePlus™ systems, using SYBR® Premix Ex Taq™ (TaKaRa) and the following thermal profile: 95°C for 3 min, and 40 cycles of 95°C, 10 sec; and 58°C, 30 sec. Primers are listed in Supplementary Table S2. *actb1* was used as an internal control. Relative mRNA expression levels were quantified using the comparative Ct ($\Delta\Delta C_t$) method and expressed as $2^{-(\Delta\Delta C_t)}$. Each PCR assay was done with three biological samples.

Construction of the expression vectors

The *alad* and *cpox* ORF (open reading frame) cDNAs were PCR amplified using zebrafish larvae (120hpf) cDNAs as template, then cloned to pcDNA3.1+, and named *alad*-pcDNA3.1 and *cpox*-pcDNA3.1, respectively. Primers for *alad* and *cpox* ORF cloning are listed in Supplementary Table S2. The human *ALAD* and *CPOX* ORF cDNAs were PCR amplified using the NIH 293T cells' cDNAs as template, and then

422 cloned to pcDNA3.1+, and named *ALAD*-pcDNA3.1 and *CPOX*-pcDNA3.1,
423 respectively. The mutated ORF cDNAs of human *ALAD* (C⁷¹⁸-T,)(Ishida et al., 1992)
424 and *CPOX* (G⁵⁸⁹-T)(Rosipal et al., 1999) were generated with Q5[®] Site-Directed
425 Mutagenesis Kit (NEB) using *ALAD*-pcDNA3.1 and *CPOX*-pcDNA3.1, respectively.

426 **Rescue experiments and *o*-dianisidine staining**

427 The plasmids of expression vectors *alad*-pcDNA3.1, *cpx*-pcDNA3.1,
428 *ALAD*-pcDNA3.1 and *CPOX*-pcDNA3.1 were linearized, and used as templates for
429 generating capped mRNAs with mMESSAGE mMACHINE[®] Kit according to the
430 manufacturer's instructions (Ambion). A mixture of capped mRNA in Tris-HCl
431 (0.01M, pH7.0) were microinjected into one-cell zebrafish embryos. Microinjection
432 controls with the vehicle solution free of mRNAs also were performed. Embryos were
433 collected at 48hpf for the *o*-dianisidine staining. Detection of hemoglobin by
434 *o*-dianisidine was performed as described previously (Ransom et al., 1996). The images
435 were acquired with a stereomicroscope microscope (Leica M165 FC) and a digital
436 camera.

437 **Blood smears assay, Wright staining and heme level determination**

438 We obtained embryonic blood cells and performed Wright staining as described
439 previously (Brownlie et al., 1998; Hanaoka et al., 2006). Embryos were bled by tail
440 amputation and immediately spread on glass slides, allowed to air dry and stained with
441 wright's dye for 10 minutes, then washed with 1 X PBS. The images were acquired with
442 a stereomicroscope microscope (Olympus U-HGLGPS) and a digital camera.
443 Circulating blood cells maintained in 1 X PBS were collected from 20 embryos and

were counted. The heme level assay was performed with the QuantiChrom™ Heme Assay Kit (BioAssay Systems).

Whole-mount *in situ* hybridization and HE (hematoxylin-eosin) staining

Whole-mount *in situ* hybridization experiments were conducted as described previously (Wang et al., 2007). Following the whole-embryo *o*-dianisidine staining, selected embryos were rehydrated in 30% sucrose at 4°C overnight for cryostat sectioning. Frozen embryos were sectioned to 8 µm thickness, and hematoxylin-eosin staining was performed as standard protocol. Sections were photographed using a stereomicroscope (Leica M165 FC) with a digital camera, and the images were analyzed by using ImageJ (National Institutes of Health).

HPLC (High-performance liquid chromatography) assay

For the ALA assay, approximately 300 larvae each for *alad*^{-/-} and WT control were collected at 7 days postfertilization (dpf) for HPLC assay. These larvae were then promptly rinsed and homogenized in 10 mM HEPES buffer for ALA assay as previously described (Costa et al., 1997). HPLC assay was conducted using 5-Aminolevulinic acid hydrochloride (Sigma) as ALA standard.

For the CP assay, approximately 300 zebrafish larvae at 7 dpf were pulverized into fine powder and homogenized in 1 mL 0.2 M HCl aqueous solution by a tissue grinder. The porphyrins were extracted twice into ether as described (Dailey et al., 2015). The extracts were combined and dried under a stream of nitrogen. Standards and samples were resuspended in 100 µl of ethyl acetate/acetic acid (4/1, v/v). The compounds are separated by liquid chromatography on the Accela LC Systems (Thermo Fisher

Scientific, San Jose, CA) using a Hypersil GOLD column (3 μ m, 150 \times 2.1 mm, Part Number: 25003-152130, Thermo Fisher Scientific). Chromatographic separation was conducted in binary gradient using 0.1% formic acid in water as mobile phase A and 0.1% formic acid in methanol as mobile phase B. The gradient elution program started at 40% B for 5 min, increased to 100% B over 7 min, where it was then held for 6 min before returning to 40% B. The flow rate was 0.2 mL/min. MS analysis of Coproporphyrin III was performed on a TSQ Vantage mass spectrometer (Thermo Fisher Scientific) in positive mode using SRM as described (Fyrestam et al., 2015). Coproporphyrinogen III (Frontier Scientific) was used as CP standard (Tomokuni et al., 1987).

Statistical analysis

The data were analyzed with unpaired, two-tailed Student's *t*-test with Microsoft Excel and the results were shown as mean \pm SD. The level of significance was accepted at $P < 0.05$. *, ** and *** represent $P < 0.05$, $P < 0.01$ and $P < 0.001$, respectively.

ACKNOWLEDGEMENTS

We thank Bo Zhang and Wenbiao Chen for providing vectors for TALEN and CRISPR-Cas9; Yi-Lin Yan and members of our laboratory for helpful comments and suggestions on this study.

Competing interests

The authors declare no competing financial interests.

Author contributions

H.W. and S.Z. conceived and designed the experiments. S.Z., J.M., Z.N., and J.W. performed the experiments. Y.H. and X.S. helped measure CP contents. Y.Z. provided reagents. S.Z. and H.W. analyzed the data and wrote the paper.

Funding

This work was supported by the grants from the National Natural Science Foundation of China (NSFC) (#81570171, #81070455, #31030062), National Basic Research Program of China (973 Program) (# 2012CB947600), National High Technology Research and Development Program of China (863 Program) (#2011AA100402-2), the Jiangsu Distinguished Professorship Program (#SR13400111), and the Natural Science Foundation of Jiangsu Province (#BK2012052), the Priority Academic Program Development (PAPD) of Jiangsu Higher Education Institutions (#YX13400214), the High-Level Innovative Team of Jiangsu Province, and the “333” Project of Jiangsu Province (BRA2015328).

Supplementary materials

Supplementary materials available online at

Reference

- Applegate, L. A., Luscher, P. and Tyrrell, R. M. (1991). Induction of heme oxygenase: a general response to oxidant stress in cultured mammalian cells. *Cancer Res* **51**, 974-8.
- Balwani, M. and Desnick, R. J. (2012). The porphyrias: advances in diagnosis and treatment. *Blood* **120**, 4496-504.
- Brownlie, A., Donovan, A., Pratt, S. J., Paw, B. H., Oates, A. C., Brugnara, C., Witkowska, H.

516 **E., Sassa, S. and Zon, L. I.** (1998). Positional cloning of the zebrafish sauternes gene: a model for
517 congenital sideroblastic anaemia. *Nat Genet* **20**, 244-50.

518 **Cappellini, M. D., Brancaloni, V., Graziadei, G., Tavazzi, D. and Di Pierro, E.** (2010).
519 Porphyrrias at a glance: diagnosis and treatment. *Intern Emerg Med* **5 Suppl 1**, S73-80.

520 **Chiabrando, D., Mercurio, S. and Tolosano, E.** (2014). Heme and erythropoiesis: more than a
521 structural role. *Haematologica* **99**, 973-83.

522 **Childs, S., Weinstein, B. M., Mohideen, M. A., Donohue, S., Bonkovsky, H. and Fishman, M.**
523 **C.** (2000). Zebrafish dracula encodes ferrochelatase and its mutation provides a model for erythropoietic
524 protoporphyria. *Curr Biol* **10**, 1001-4.

525 **Cong, L. and Zhang, F.** (2015). Genome engineering using CRISPR-Cas9 system. *Methods Mol*
526 *Biol* **1239**, 197-217.

527 **Costa, C. A., Trivelato, G. C., Demasi, M. and Bechara, E. J.** (1997). Determination of
528 5-aminolevulinic acid in blood plasma, tissues and cell cultures by high-performance liquid
529 chromatography with electrochemical detection. *J Chromatogr B Biomed Sci Appl* **695**, 245-50.

530 **Dailey, H. A., Gerdes, S., Dailey, T. A., Burch, J. S. and Phillips, J. D.** (2015). Noncanonical
531 coproporphyrin-dependent bacterial heme biosynthesis pathway that does not use protoporphyrin. *Proc*
532 *Natl Acad Sci U S A* **112**, 2210-5.

533 **Detrich, H. W., 3rd, Kieran, M. W., Chan, F. Y., Barone, L. M., Yee, K., Rundstadler, J. A.,**
534 **Pratt, S., Ransom, D. and Zon, L. I.** (1995). Intraembryonic hematopoietic cell migration during
535 vertebrate development. *Proc Natl Acad Sci U S A* **92**, 10713-7.

536 **Dooley, K. and Zon, L. I.** (2000). Zebrafish: a model system for the study of human disease. *Curr*
537 *Opin Genet Dev* **10**, 252-6.

538 **Dooley, K. A., Fraenkel, P. G., Langer, N. B., Schmid, B., Davidson, A. J., Weber, G., Chiang,**
539 **K., Foott, H., Dwyer, C., Wingert, R. A. et al.** (2008). montalcino, A zebrafish model for variegate
540 porphyria. *Exp Hematol* **36**, 1132-42.

541 **Doyle, E. L., Booher, N. J., Standage, D. S., Voytas, D. F., Brendel, V. P., Vandyk, J. K. and**
542 **Bogdanove, A. J.** (2012). TAL Effector-Nucleotide Targeter (TALE-NT) 2.0: tools for TAL effector
543 design and target prediction. *Nucleic Acids Res* **40**, W117-22.

544 **Furutani-Seiki, M. and Wittbrodt, J.** (2004). Medaka and zebrafish, an evolutionary twin study.
545 *Mech Dev* **121**, 629-37.

546 **Furuyama, K., Kaneko, K. and Vargas, P. D.** (2007). Heme as a magnificent molecule with
547 multiple missions: heme determines its own fate and governs cellular homeostasis. *Tohoku J Exp Med*
548 **213**, 1-16.

549 **Fyrestam, J., Bjurshammar, N., Paulsson, E., Johannsen, A. and Ostman, C.** (2015).
550 Determination of porphyrins in oral bacteria by liquid chromatography electrospray ionization tandem
551 mass spectrometry. *Anal Bioanal Chem* **407**, 7013-23.

552 **Ged, C., Mendez, M., Robert, E., Lalanne, M., Lamrissi-Garcia, I., Costet, P., Daniel, J. Y.,**
553 **Dubus, P., Mazurier, F., Moreau-Gaudry, F. et al.** (2006). A knock-in mouse model of congenital
554 erythropoietic porphyria. *Genomics* **87**, 84-92.

555 **Hanaoka, R., Katayama, S., Dawid, I. B. and Kawahara, A.** (2006). Characterization of the
556 heme synthesis enzyme coproporphyrinogen oxidase (CPO) in zebrafish erythrocytes. *Genes Cells* **11**,
557 293-303.

558 **Hsu, P. D., Lander, E. S. and Zhang, F.** (2014). Development and applications of CRISPR-Cas9
559 for genome engineering. *Cell* **157**, 1262-78.

560 **Huang, P., Xiao, A., Tong, X., Zu, Y., Wang, Z. and Zhang, B.** (2014). TALEN construction via
561 "Unit Assembly" method and targeted genome modifications in zebrafish. *Methods* **69**, 67-75.

562 **Hwang, W. Y., Fu, Y., Reyon, D., Maeder, M. L., Tsai, S. Q., Sander, J. D., Peterson, R. T., Yeh,
563 J. R. and Joung, J. K.** (2013). Efficient genome editing in zebrafish using a CRISPR-Cas system. *Nat*
564 *Biotechnol* **31**, 227-9.

565 **Igarashi, K. and Sun, J.** (2006). The heme-Bach1 pathway in the regulation of oxidative stress
566 response and erythroid differentiation. *Antioxid Redox Signal* **8**, 107-18.

567 **Irion, U., Krauss, J. and Nusslein-Volhard, C.** (2014). Precise and efficient genome editing in
568 zebrafish using the CRISPR/Cas9 system. *Development* **141**, 4827-30.

569 **Ishida, N., Fujita, H., Fukuda, Y., Noguchi, T., Doss, M., Kappas, A. and Sassa, S.** (1992).
570 Cloning and expression of the defective genes from a patient with delta-aminolevulinic acid dehydratase
571 porphyria. *J Clin Invest* **89**, 1431-7.

572 **Jaffe, E. K. and Stith, L.** (2007). ALAD porphyria is a conformational disease. *Am J Hum Genet*
573 **80**, 329-37.

574 **Kuhnel, A., Gross, U. and Doss, M. O.** (2000). Hereditary coproporphyria in Germany:
575 clinical-biochemical studies in 53 patients. *Clin Biochem* **33**, 465-73.

576 **Lamoril, J., Martasek, P., Deybach, J. C., Da Silva, V., Grandchamp, B. and Nordmann, Y.**
577 (1995). A molecular defect in coproporphyrinogen oxidase gene causing harderoporphyria, a variant
578 form of hereditary coproporphyria. *Hum Mol Genet* **4**, 275-8.

579 **Lieschke, G. J. and Currie, P. D.** (2007). Animal models of human disease: zebrafish swim into
580 view. *Nat Rev Genet* **8**, 353-67.

581 **Lindberg, R. L., Porcher, C., Grandchamp, B., Ledermann, B., Burki, K., Brandner, S.,
582 Aguzzi, A. and Meyer, U. A.** (1996). Porphobilinogen deaminase deficiency in mice causes a
583 neuropathy resembling that of human hepatic porphyria. *Nat Genet* **12**, 195-9.

584 **MacRae, C. A. and Peterson, R. T.** (2015). Zebrafish as tools for drug discovery. *Nat Rev Drug*
585 *Discov* **14**, 721-31.

586 **Martasek, P., Camadro, J. M., Raman, C. S., Lecomte, M. C., Le Caer, J. P., Demeler, B.,
587 Grandchamp, B. and Labbe, P.** (1997). Human coproporphyrinogen oxidase. Biochemical
588 characterization of recombinant normal and R231W mutated enzymes expressed in E. coli as soluble,
589 catalytically active homodimers. *Cell Mol Biol (Noisy-le-grand)* **43**, 47-58.

590 **Maruno, M., Furuyama, K., Akagi, R., Horie, Y., Meguro, K., Garbaczewski, L., Chiorazzi,
591 N., Doss, M. O., Hassoun, A., Mercelis, R. et al.** (2001). Highly heterogeneous nature of
592 delta-aminolevulinic acid dehydratase (ALAD) deficiencies in ALAD porphyria. *Blood* **97**, 2972-8.

593 **Medlock, A. E., Meissner, P. N., Davidson, B. P., Corrigall, A. V. and Dailey, H. A.** (2002). A
594 mouse model for South African (R59W) variegate porphyria: construction and initial characterization.
595 *Cell Mol Biol (Noisy-le-grand)* **48**, 71-8.

596 **Meissner, P. N., Dailey, T. A., Hift, R. J., Ziman, M., Corrigall, A. V., Roberts, A. G., Meissner,
597 D. M., Kirsch, R. E. and Dailey, H. A.** (1996). A R59W mutation in human protoporphyrinogen
598 oxidase results in decreased enzyme activity and is prevalent in South Africans with variegate porphyria.
599 *Nat Genet* **13**, 95-7.

600 **Mori, M., Gotoh, S., Taketani, S., Hiai, H. and Higuchi, K.** (2013). Hereditary cataract of the
601 Nakano mouse: Involvement of a hypomorphic mutation in the coproporphyrinogen oxidase gene. *Exp*
602 *Eye Res* **112**, 45-50.

603 **Nordmann, Y., Grandchamp, B., de Verneuil, H., Phung, L., Cartigny, B. and Fontaine, G.**

(1983). Harderoporphyria: a variant hereditary coproporphyria. *J Clin Invest* **72**, 1139-49.

North, T. E., Goessling, W., Walkley, C. R., Lengerke, C., Kopani, K. R., Lord, A. M., Weber, G. J., Bowman, T. V., Jang, I. H., Grosser, T. et al. (2007). Prostaglandin E2 regulates vertebrate haematopoietic stem cell homeostasis. *Nature* **447**, 1007-11.

Phillips, J. D., Jackson, L. K., Bunting, M., Franklin, M. R., Thomas, K. R., Levy, J. E., Andrews, N. C. and Kushner, J. P. (2001). A mouse model of familial porphyria cutanea tarda. *Proc Natl Acad Sci U S A* **98**, 259-64.

Pouretzadi, S. J., Donahue, E. K. and Wingert, R. A. (2014). A Manual Small Molecule Screen Approaching High-throughput Using Zebrafish Embryos. *J Vis Exp*.

Puy, H., Gouya, L. and Deybach, J. C. (2010). Porphyrias. *Lancet* **375**, 924-37.

Ransom, D. G., Haffter, P., Odenthal, J., Brownlie, A., Vogelsang, E., Kelsh, R. N., Brand, M., van Eeden, F. J., Furutani-Seiki, M., Granato, M. et al. (1996). Characterization of zebrafish mutants with defects in embryonic hematopoiesis. *Development* **123**, 311-9.

Rennekamp, A. J. and Peterson, R. T. (2015). 15 years of zebrafish chemical screening. *Curr Opin Chem Biol* **24**, 58-70.

Rosipal, R., Lamoril, J., Puy, H., Da Silva, V., Gouya, L., De Rooij, F. W., Te Velde, K., Nordmann, Y., Martasek, P. and Deybach, J. C. (1999). Systematic analysis of coproporphyrinogen oxidase gene defects in hereditary coproporphyria and mutation update. *Hum Mutat* **13**, 44-53.

Ryter, S. W. and Tyrrell, R. M. (2000). The heme synthesis and degradation pathways: role in oxidant sensitivity. Heme oxygenase has both pro- and antioxidant properties. *Free Radic Biol Med* **28**, 289-309.

Sakamoto, D., Kudo, H., Inohaya, K., Yokoi, H., Narita, T., Naruse, K., Mitani, H., Araki, K., Shima, A., Ishikawa, Y. et al. (2004). A mutation in the gene for delta-aminolevulinic acid dehydratase (ALAD) causes hypochromic anemia in the medaka, *Oryzias latipes*. *Mech Dev* **121**, 747-52.

Santoriello, C. and Zon, L. I. (2012). Hooked! Modeling human disease in zebrafish. *J Clin Invest* **122**, 2337-43.

Siegesmund, M., van Tuyl van Serooskerken, A. M., Poblete-Gutierrez, P. and Frank, J. (2010). The acute hepatic porphyrias: current status and future challenges. *Best Pract Res Clin Gastroenterol* **24**, 593-605.

Tahara, T., Sun, J., Igarashi, K. and Taketani, S. (2004a). Heme-dependent up-regulation of the alpha-globin gene expression by transcriptional repressor Bach1 in erythroid cells. *Biochem Biophys Res Commun* **324**, 77-85.

Tahara, T., Sun, J., Nakanishi, K., Yamamoto, M., Mori, H., Saito, T., Fujita, H., Igarashi, K. and Taketani, S. (2004b). Heme positively regulates the expression of beta-globin at the locus control region via the transcriptional factor Bach1 in erythroid cells. *J Biol Chem* **279**, 5480-7.

Tomokuni, K., Ichiba, M., Hirai, Y. and Hasegawa, T. (1987). Optimized liquid-chromatographic method for fluorometric determination of urinary delta-aminolevulinic acid in workers exposed to lead. *Clin Chem* **33**, 1665-7.

Tutois, S., Montagutelli, X., Da Silva, V., Jouault, H., Rouyer-Fessard, P., Leroy-Viard, K., Guenet, J. L., Nordmann, Y., Beuzard, Y. and Deybach, J. C. (1991). Erythropoietic protoporphyria in the house mouse. A recessive inherited ferrochelatase deficiency with anemia, photosensitivity, and liver disease. *J Clin Invest* **88**, 1730-6.

Tzou, W. S., Chu, Y., Lin, T. Y., Hu, C. H., Pai, T. W., Liu, H. F., Lin, H. J., Cases, I., Rojas, A., Sanchez, M. et al. (2014). Molecular evolution of multiple-level control of heme biosynthesis pathway

648 in animal kingdom. *PLoS One* **9**, e86718.

649 **Wang, H., Long, Q., Marty, S. D., Sassa, S. and Lin, S.** (1998). A zebrafish model for
650 hepatoerythropoietic porphyria. *Nat Genet* **20**, 239-43.

651 **Wang, H., Zhou, Q., Kesinger, J. W., Norris, C. and Valdez, C.** (2007). Heme regulates exocrine
652 peptidase precursor genes in zebrafish. *Exp Biol Med (Maywood)* **232**, 1170-80.

653 **Wei, C., Liu, J., Yu, Z., Zhang, B., Gao, G. and Jiao, R.** (2013). TALEN or Cas9 - rapid, efficient
654 and specific choices for genome modifications. *J Genet Genomics* **40**, 281-9.

655 **Weinstein, B. M., Schier, A. F., Abdelilah, S., Malicki, J., Solnica-Krezel, L., Stemple, D. L.,
656 Stainier, D. Y., Zwartkruis, F., Driever, W. and Fishman, M. C.** (1996). Hematopoietic mutations in
657 the zebrafish. *Development* **123**, 303-9.

658 **Whatley, S. D., Mason, N. G., Woolf, J. R., Newcombe, R. G., Elder, G. H. and Badminton, M.
659 N.** (2009). Diagnostic strategies for autosomal dominant acute porphyrias: retrospective analysis of 467
660 unrelated patients referred for mutational analysis of the HMBS, CPOX, or PPOX gene. *Clin Chem* **55**,
661 1406-14.

662 **Xiao, A., Wang, Z., Hu, Y., Wu, Y., Luo, Z., Yang, Z., Zu, Y., Li, W., Huang, P., Tong, X. et al.**
663 (2013). Chromosomal deletions and inversions mediated by TALENs and CRISPR/Cas in zebrafish.
664 *Nucleic Acids Res* **41**, e141.

665 **Yano, Y. and Kondo, M.** (1998). [ALAD deficiency porphyria (ADP)]. *Ryoikibetsu Shokogun
666 Shirizu*, 139-40.

667 **Zhang, S., Xu, M., Huang, J., Tang, L., Zhang, Y., Wu, J., Lin, S. and Wang, H.** (2014). Heme
668 acts through the Bach1b/Nrf2a-MafK pathway to regulate exocrine peptidase precursor genes in
669 porphyric zebrafish. *Dis Model Mech* **7**, 837-45.

670 **Zon, L. I. and Peterson, R. T.** (2005). In vivo drug discovery in the zebrafish. *Nat Rev Drug
671 Discov* **4**, 35-44.

678

Table 1. Animal models for human porphyrias

Human disease	Gene	Animal model	Species
ALA dehydratase deficient porphyria	ALAD	<i>whiteout</i> <i>alad</i>	Medaka Zebrafish
Acute intermittent porphyria	HMBS	T1/T2(-/-)	Mouse
Congenital erythropoietic porphyria	UROS	<i>Uros^{mut248}</i>	Mouse
Porphyria cutanea tarda /hepatoerythropoietic porphyria	UROD	<i>yquem</i> <i>URO-D+/-</i>	Zebrafish Mouse
Hereditary coproporphyria	CPOX	Nakano <i>cpx</i>	Mouse Zebrafish
Variegate porphyria	PPOX	<i>Montalcino</i> Human R59W mutation Knock-in	Zebrafish Mouse
Erythropoietic protoporphyria	FECH	<i>dracula</i> BALB/c <i>Fech^{m1Pas}</i>	Zebrafish Mouse

679

680

681

682 **Figure legends**

683 **Fig. 1. TALEN and CRISPR-Cas9 targeted sites and mutated sequences. (A)**

684 TALENs were designed to target the third exon of the zebrafish *alad* gene. The
685 wild-type (WT) sequence with the two TALEN arms is highlighted in blue, and the
686 BsmA I restriction endonuclease site for genotyping is underlined. (B) WT sequence
687 and F₀ mutated sequence with indels at the *alad* TALEN-targeted fragment. (C) A
688 *alad* mutant line contains a 14-bp deletion resulting in a frame shift starting at the 51st
689 amino acid. (D) A 20-nt gRNA was designed to target the second exon of the zebrafish
690 *cpox* gene. The WT sequence with the PAM is highlighted in blue, and the Hinf I
691 restriction endonuclease site for genotyping is underlined. (E) WT sequence and F₀
692 mutated sequences with indels at the *cpox* CRISPR-Cas9-targeted fragment. (F) Two
693 *cpox* mutant lines, one containing a 6-bp deletion resulting in deletion of the 2 amino
694 acids (210 Leu and 211 Thr) and the other having a 11-bp deletion resulting a
695 truncated peptide with only 208 amino acids.

696 **Fig. 2. Phenotypes of homozygous mutants with mutated *alad* and *cpox* genes. (A)**

697 Lateral views of WT, *alad*^{-/-} and *cpox*^{-/-} (6-bp deletion) zebrafish embryos at 48 hpf.
698 Arrows indicate the pericardium. (B) Lateral views of WT, *alad*^{-/-} and *cpox*^{-/-} (6-bp
699 deletion) zebrafish larvae at 10 dpf. (C) Body lengths of *alad*^{-/-} and *cpox*^{-/-} (6-bp
700 deletion) larvae at 10 dpf compared with wild types. 25 larvae per group were
701 measured for statistical analysis. Student's *t*-tests were conducted. ***P<0.001. (D)
702 Survival rate of *alad*^{-/-} and *cpox*^{-/-} (6-bp deletion) from 1 dpf to 13d pf compared with
703 wild types. 40 larvae per group were examined for statistical analysis. (E) *In situ*

704 hybridization staining shows the down-regulation of *slc4a1a* in *alad*^{-/-} and *cpox*^{-/-}
705 (11-bp deletion) embryos at 48 hpf. (F) Mean optic densities of *in situ* hybridization
706 staining of a group of larvae (10-12 each) corresponding to Fig. 2E were quantified by
707 using ImageJ. Student's *t*-tests were conducted. *P<0.05. (G) qRT-PCR analysis
708 shows down-regulation of *slc4a1a* in *alad*^{-/-} and *cpox*^{-/-} (11-bp deletion). Student's
709 *t*-tests were conducted. *P<0.05.

710 **Fig. 3. Abnormality of blood cells in *alad*^{-/-} and *cpxo*^{-/-} mutants.** Whole-mount
711 *o*-dianisidine staining of WT (A, D and G), *alad*^{-/-} (B, E and H) and *cpxo*^{-/-} (6-bp
712 deletion) (C, F and I) embryos at 32 hpf (A, B and C), 48 hpf (D, E and F), and 72 hpf
713 (G, H and I). Shown are ventral views. (J) Statistical analysis of optic densities of
714 whole-mount *o*-dianisidine staining, shown in A, B, C, D, E, F, G, H and I, measured
715 by ImageJ. 20 embryos per group were measured for statistical analysis. Student's
716 *t*-tests were conducted. *P<0.05, **P<0.01, ***P<0.001. (K) Relative mRNA levels
717 of *hbae1* and *hbbe2* in WT, *alad*^{-/-} and *cpxo*^{-/-} (6-bp deletion) embryos at 48hpf.
718 Circulating red blood cells of WT (L, O and R), *alad*^{-/-} (M, P and S) and *cpxo*^{-/-} (6-bp
719 deletion) (N, Q and T) embryos/larvae at 36 hpf (L, M and N), 72 hpf (O, P and Q),
720 and 108 hpf (R, S and T) with Wright staining. (U) Statistical analysis of optic nuclear
721 areas shown in L, M, N, O, P, Q, R, S, and T. The nuclei of *alad*^{-/-} and *cpox*^{-/-} (6-bp
722 deletion) are larger than those of WT at 72 hpf and 108 hpf. Optic nuclear areas were
723 measured by ImageJ. 30 blood cells per group were measured for statistical analysis.
724 Student's *t*-tests were conducted. ***P<0.001. (V) Relative heme levels of circulating

725 red blood cells in WT, *alad*^{-/-} and *cpox*^{-/-} (6-bp deletion) embryos at 7 dpf,
 726 determined by the QuantiChrom™ Heme Assay Kit.

727 **Fig. 4. Accumulation of metabolic intermediates in *alad*^{-/-} and *cpox*^{-/-} mutants.**

728 (A) ALA measurements with HPLC (High-performance liquid chromatography) in
 729 WT and *alad*^{-/-} larvae at 7 dpf. Relative fluorescence of ALA peak in WT and *alad*^{-/-}.
 730 (B) CP measurements with HPLC in WT and *cpox*^{-/-} (11-bp deletion) larvae at 7 dpf.
 731 Relative fluorescence of CP peak in WT and *cpox*^{-/-} (11-bp deletion). Reddish
 732 autofluorescence of *cpox*^{-/-} embryo at 32 hpf (C, D), the top embryo is *cpox*^{-/-}
 733 mutants, the bottom one is the wild-type siblings. (C) Bright light image. (D) Image
 734 under a fluorescent microscope with a rhodamine filter. The arrow indicates
 735 autofluorescence of the yolk sac of the *cpox*^{-/-} (6-bp deletion) embryo.

736 Autofluorescence analysis of larvae of wild-type (E, F), *urod*^{-/-} (G, H), *cpox*^{-/-} (6-bp
 737 deletion) (I, J), *ppox*^{-/-} (L, L) and *fech*^{-/-} (M, N) at 72hpf. (E, G, I, K and M), Bright
 738 light image. (F, H, J, L and N) Image under a fluorescent microscope with a
 739 rhodamine filter.

740 **Fig. 5. Rescuing the phenotypes of zebrafish *alad*^{-/-} and *cpox*^{-/-} mutants by**
 741 **zebrafish and human genes.** (A) Whole-mount *o*-dianisidine staining of wild-type
 742 embryos, *alad*^{-/-} embryos, *alad*^{-/-} embryos injected with zebrafish *alad* mRNA and
 743 *alad*^{-/-} embryos injected with human *ALAD* mRNA at 48 hpf. (B) Statistical analysis
 744 of optic densities measured by ImageJ. 25 embryos per group were measured for
 745 statistical analysis. Student's *t*-tests were conducted. *P<0.05, ***P<0.001. (C)
 746 Whole-mount *o*-dianisidine staining of wild-type embryos, *cpox*^{-/-} (6-bp deletion)

747 embryos, *cpox*^{-/-} (6-bp deletion) embryos injected with zebrafish *cpox* mRNA and
 748 *cpox*^{-/-} embryos injected with human *CPOX* mRNA at 48 hpf. (D) Statistical analysis
 749 of optic blood cells about C. Optic densities were measured by ImageJ, 20 embryos
 750 per group were measured for statistical analysis. Student's *t*-tests were conducted.
 751 *P<0.05, ***P<0.001.

752 **Fig. 6. Altered expression of genes involved in heme biosynthesis and degradation,**
 753 **and exocrine pancreatic zymogens in *alad*^{-/-} and *cpox*^{-/-} mutants detected by**
 754 **qRT-PCR analysis.** (A) Altered expression of genes involved in heme biosynthesis
 755 including *alas1*, *alas2*, *alad*, *hmbsa* and *hmsb* in *alad*^{-/-} at 48 hpf. (B) Altered
 756 expression of genes involved in heme biosynthesis including *alas1*, *alas2*, *urod*, *cpox*
 757 and *ppox* in *cpox*^{-/-} (6-bp deletion) at 48 hpf. (C) Altered expression of genes involved
 758 in heme degradation including *hmox1*, *hmox2a* and *hmox2b* in *alad*^{-/-} and *cpox*^{-/-}
 759 (6-bp deletion) at 48 hpf. (D) Down-regulation of exocrine pancreatic zymogens in
 760 *alad*^{-/-} and *cpox*^{-/-} (6-bp deletion) at 72 hpf. Student's *t*-tests were conducted.
 761 *P<0.05, **P<0.01, ***P<0.001, n.s., not significant.

762

763

764 **Resource Impact**

765

766 **Clinical issue**

767 Heme is the prosthetic group for a number of important proteins and enzymes such as
 768 hemoglobin, catalases, and cytochromes. Heme biosynthesis is catalyzed by a cascade
 769 of highly conserved eight enzymatic reactions occurred in the mitochondria and the
 770 cytoplasm. Defects in the heme biosynthetic enzymes result in a group of human
 771 metabolic genetic disorders known as porphyrias. Using a zebrafish model for human
 772 hepatoerythropoietic porphyria (HEP), caused by defective uroporphyrinogen
 773 decarboxylase (UROD), the fifth enzyme in the heme biosynthesis pathway, we
 774 recently have found a novel aspect of porphyria pathogenesis. However, no hereditary
 775 zebrafish models with genetic mutations of *alad* and *cpox*, encoding the second
 776 enzyme delta-aminolevulinate dehydratase (ALAD) and the sixth enzyme
 777 coproporphyrinogen oxidase (CPOX), have been established to date.

778 **Results**

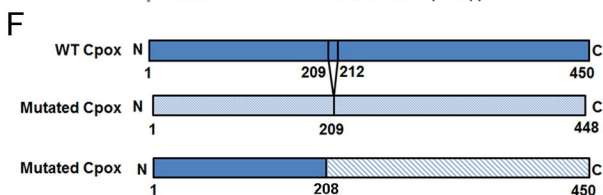
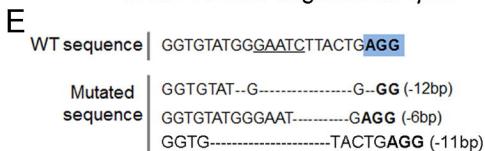
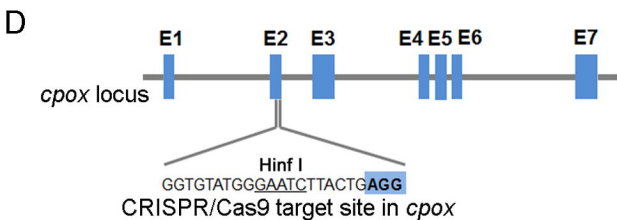
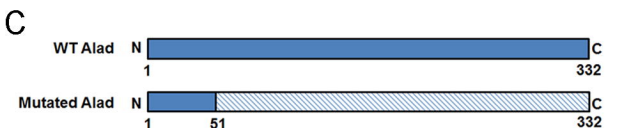
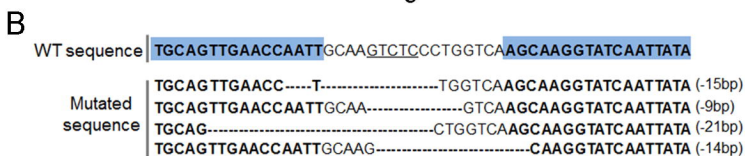
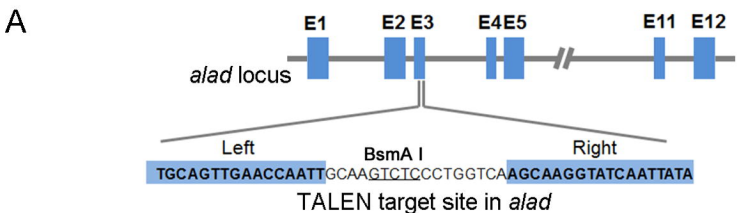
779 We employed site-specific genome-editing tools transcription activator-like effector
 780 nuclease (TALEN) and clustered regularly interspaced short palindromic repeats
 781 (CRISPR)/CRISPR-associated protein 9 (Cas9) to generate zebrafish mutants for *alad*
 782 and *cpox*. Characterization of these two zebrafish mutants revealed that they display
 783 phenotypes of heme deficiency, hypochromia, abnormal erythrocytic maturation and
 784 accumulation of heme precursor intermediates, reminiscent of human
 785 ALA-dehydratase-deficient porphyria (ADP) and hereditary coproporphyrin (HCP).

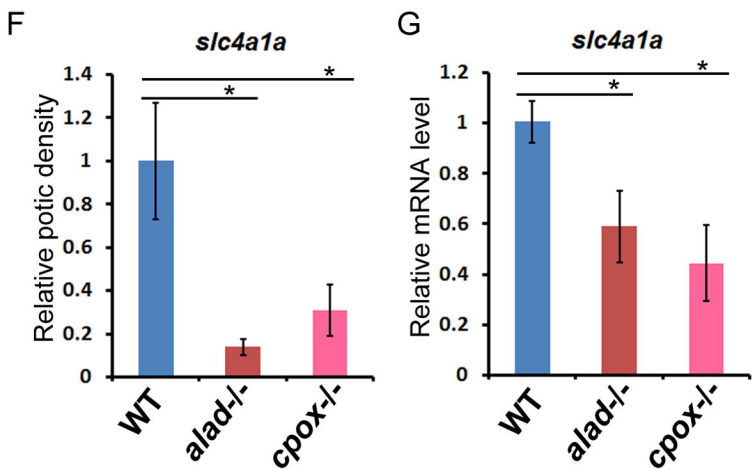
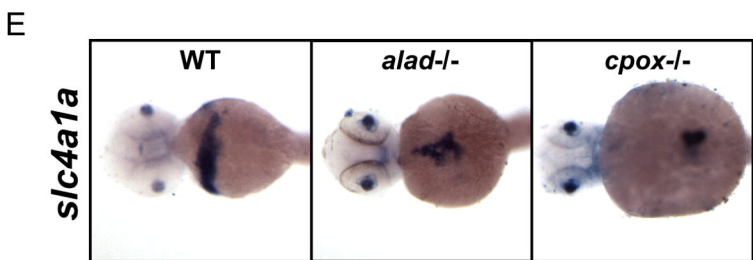
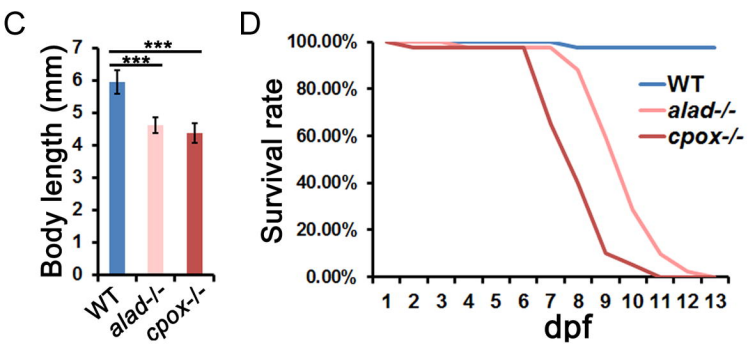
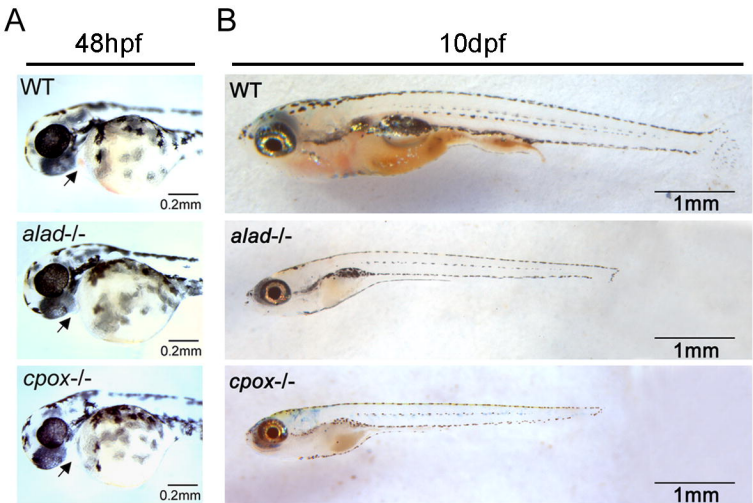
786

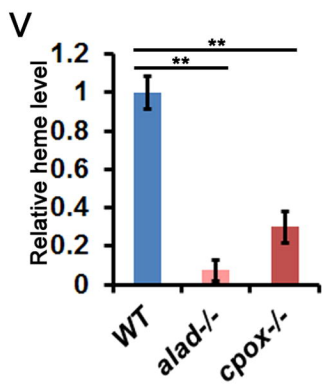
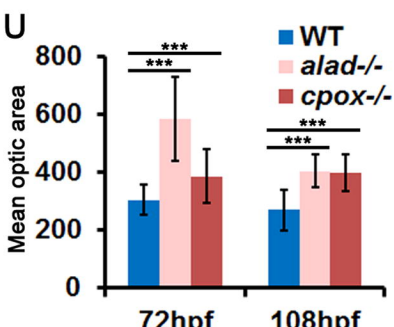
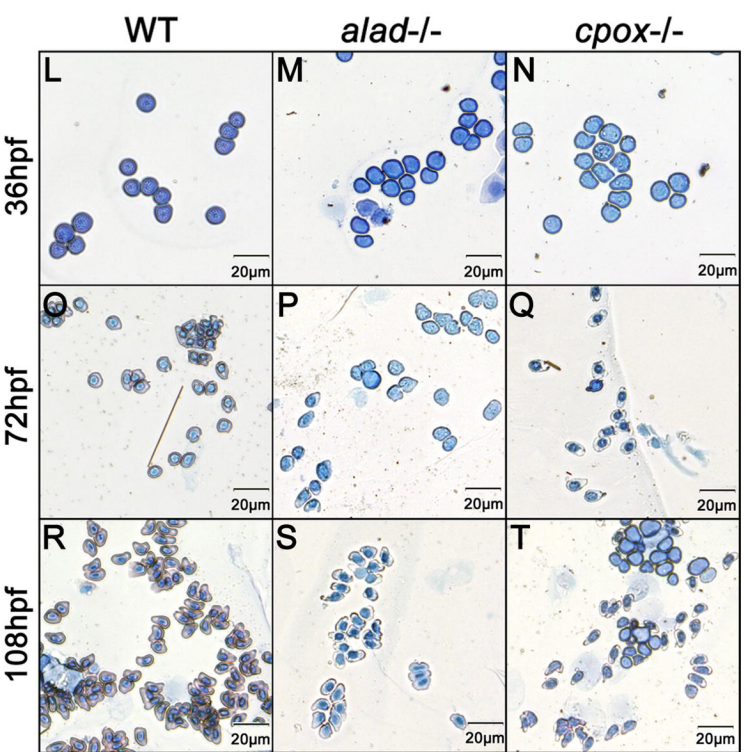
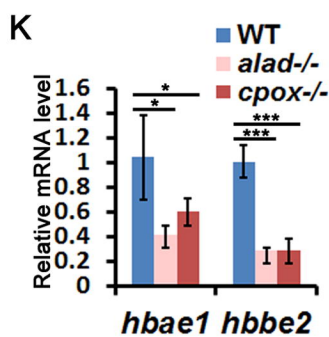
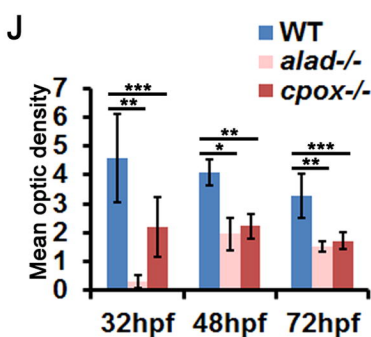
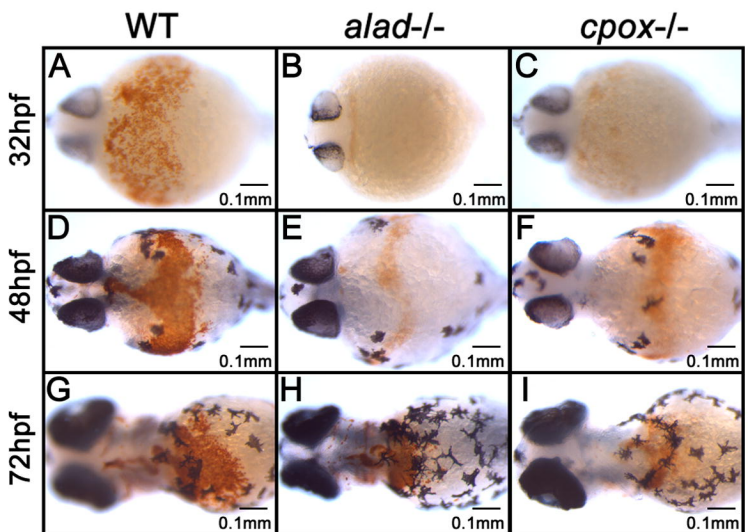
787 **Implications and future directions**

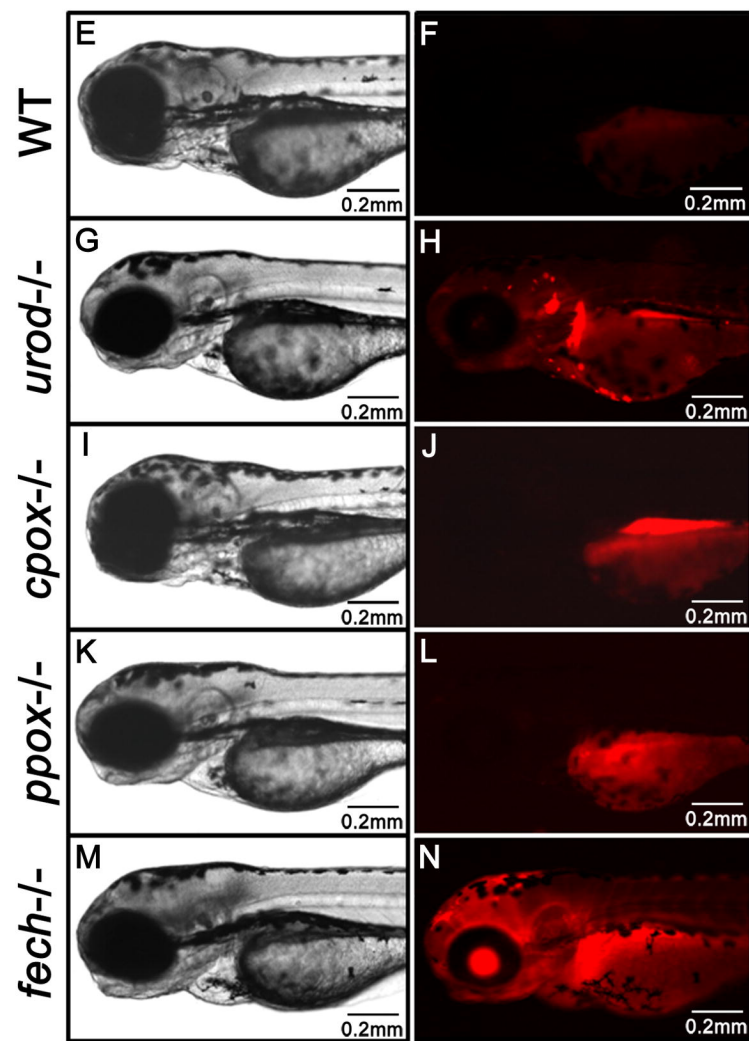
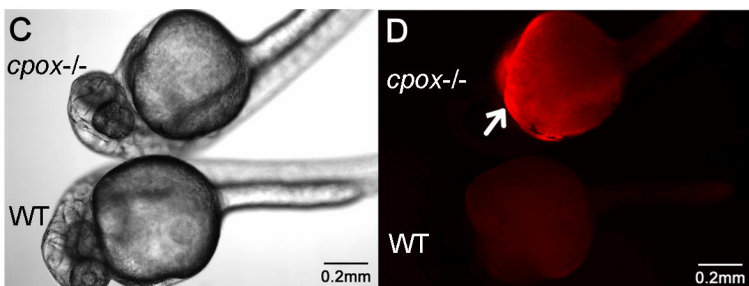
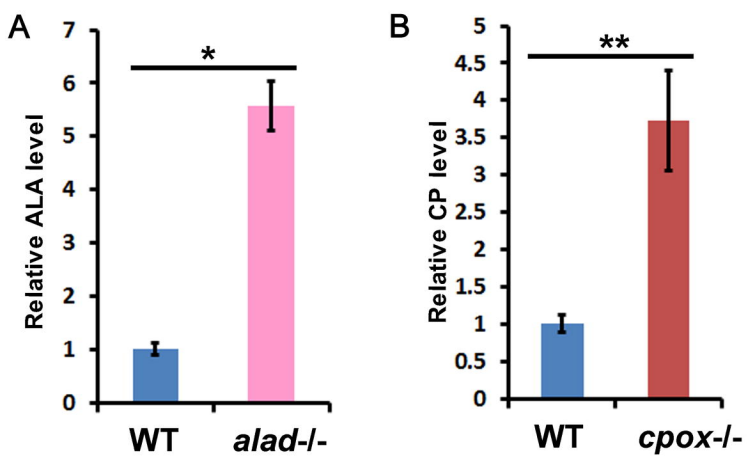
788 These two zebrafish porphyria models provide invaluable resources for elucidating
789 novel pathological aspects of porphyrias, *in vivo* tools for evaluating human mutated
790 forms of these two enzymes, discovering new therapeutic targets and developing
791 effective drugs for these complex genetic diseases. Our studies also highlight
792 generation of zebrafish models for human diseases with two new versatile
793 genome-editing tools.

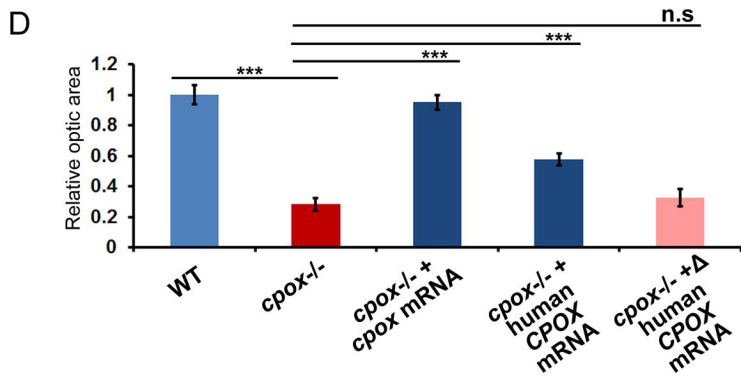
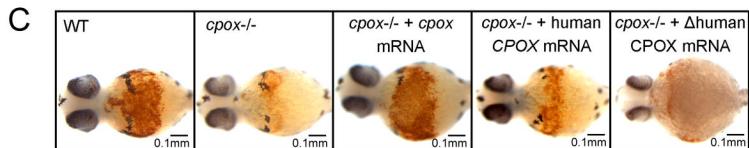
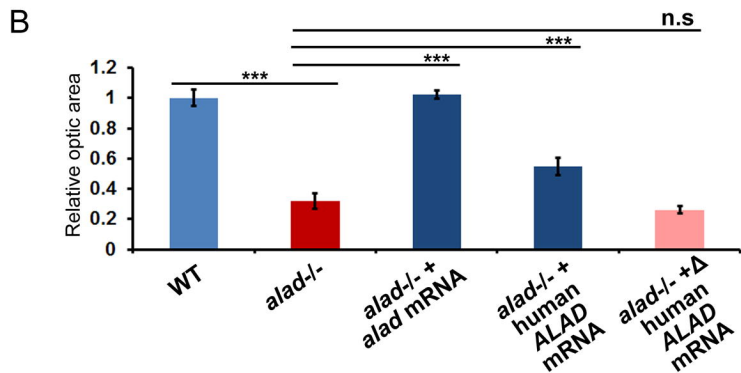
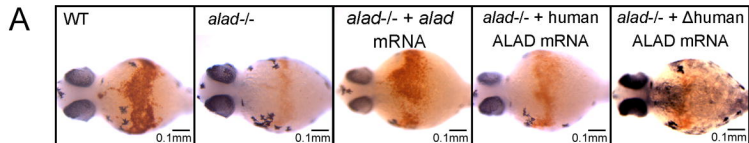
794

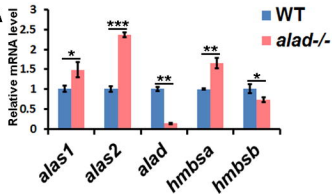
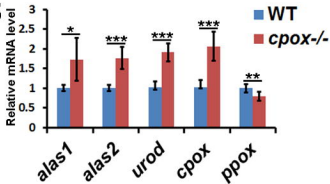
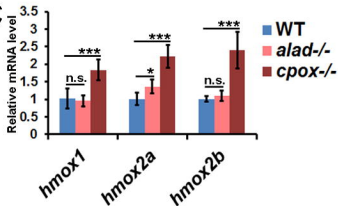










A**B****C****D**